

1 **The First Road Surface Type Dataset for 50 African
2 Countries and Regions**

3 Zixian Liu¹, Qi Zhou^{1*}, Fayong Zhang^{1*}, Prosper Basommi Laari²

4 1. *School of Geography and Information Engineering, China University of
5 Geosciences, Wuhan, People's Republic of China*

6 2. *Department of Environment and Resource Studies, Simon Diedong Dombo
7 University of Business and Integrated Development Studies, Wa, Ghana*

8 *Corresponding author: Qi Zhou (zhouqi@cug.edu.cn); Fayong Zhang
9 (zhangfayong@cug.edu.cn)

10

11 **Abstract**

12 Road surface types not only influence the accessibility of road networks and socio-
13 economic development but also serve as a critical data source for evaluating the United
14 Nations Sustainable Development Goal (SDG) 9.1. Existing research indicates that
15 **Africa generally ~~have~~has a low road paved rate, ~~limiting~~which limits local socio-**
16 economic development. Although the International Road Federation (IRF) provides
17 statistical data on paved road length and road paved rates for certain African countries,
18 this data neither covers all African ~~country~~countries nor specifies the surface type of
19 individual roads, making it challenging to ~~offer~~support decision-making ~~support~~ for
20 improving Africa's road infrastructure. To ~~fill~~address this gap, this study developed the
21 first dataset for 50 African countries and regions, incorporating the surface type of every
22 road. This was achieved using multi-source geospatial data and a tabular deep learning
23 model. The core methodology involved designing 16 proxy indicators across three
24 dimensions—derived from five open geospatial datasets (~~OSM~~OpenStreetMap road
25 data, GDP data, population distribution data, building height data, and land cover
26 data)—to infer road surface types across Africa. Key findings include: ~~The~~the accuracy
27 of the African road surface type dataset ranges from 77% to 96%, with F1 scores
28 between 0.76 and 0.96. Total road length, paved road length, and road paved rates
29 calculated from this dataset show high correlation (correlation coefficients: 0.69–0.94)
30 with corresponding IRF statistics. Notably, the road paved rate also exhibits strong
31 correlation with GNI per capita and ~~HDI~~the Human Development Index (HDI)
32 (correlation coefficients: 0.80–0.83), validating the reliability of the dataset. Spatial

设置了格式: 突出显示

33 analysis of African road paved rates at national, provincial, and county scales revealed
34 an average paved rate of only 17.4% across the 50 countries and regions. A distinct
35 ~~"pattern emerged, with higher paved rates in the north and south, and lower rates in~~
36 ~~the central region"~~ ~~pattern emerged,"~~: the average paved rate north of the Sahara is
37 approximately three times that of Sub-Saharan Africa (excluding South Africa). The
38 African road surface type dataset developed in this study not only provides data support
39 for enhancing road infrastructure and evaluating SDG 9.1 progress toward SDG 9.1 in
40 Africa but may also facilitate research on how road surface types impact road safety,
41 energy consumption, ecological environments, and socio-economic development.

42 **Keywords:** Road surface type; multi-source geospatial data; SDG 9; Africa

43

44 1. Introduction

45 Road surface types ~~(such as paved and unpaved roads)~~ not only affect vehicle
46 driving safety and energy consumption but also ~~impacts~~affect road accessibility and
47 socio-economic development (Anyanwu et al., 2009; Shtayat et al., 2020; Sha, 2021;
48 Styer J et al., 2024; Chen et al., 2025). Generally, paved roads have a ~~sturdy~~durable
49 structure and are resistant to erosion, allowing them to ~~be~~remain passable ~~all season,~~
50 ~~while~~year-round. In contrast, unpaved roads ~~may be affected~~are often impacted by
51 natural factors such as rain and snow, making them typically difficult to ~~pass all-~~
52 ~~season~~traverse throughout the year. The proportion of the rural population living within
53 2 kilometers of an all-season road has ~~also~~ been adopted by the World Bank as ~~an~~
54 ~~important~~a key indicator for evaluating road infrastructure, ~~and this~~. This indicator was

55 incorporated by the United Nations into ~~the~~-Sustainable Development Goal (SDG) 9.1
56 in 2017. ~~Read~~Data on road surface ~~type~~datatype are considered ~~one of the key data~~
57 ~~sources~~essential for assessing progress toward SDG 9.1.

58 Existing studies indicate that the road paved rate in African countries is highly
59 positively correlated with national poverty rates, ~~and~~-in some regions, the lack of all-
60 season passable roads has~~led to~~ significantly increased transportation costs (Anyanwu
61 et al., 2009; Abdulkadr et al., 2022). Particularly in Sub-Saharan Africa, more than 70%
62 of roads remain unpaved (Greening et al., 2010); In Nigeria, for example, over 30
63 million rural residents have long been unable to access road transportation services. In
64 these countries and regions, the lag in transportation infrastructure has become ~~one of~~
65 ~~the main bottlenecksa major bottleneck~~ restricting socio-economic development (Li et
66 al., 2022). To address these challenges, the World Bank, the International Automobile
67 Federation (FIA), and the International Transport Forum (ITF) signed a Memorandum
68 of Understanding (MoU) in 2018, aiming to strengthen infrastructure construction in
69 Africa over the next fifty years (World Bank, 2018). The Agenda 2063: The Africa We
70 Want, ~~participated in~~endorsed by multiple African countries, also sets goals to improve
71 residents' quality of life and enhance infrastructure ~~in African nations across the~~
72 continent (African Union Commission, 2018). Therefore, high-quality road surface
73 type data for Africa are of great significance for improving local transportation
74 infrastructure and promoting socio-economic development.

75 However, the currently available, ~~globally open road surface type~~global data ~~on~~
76 road surface types are primarily statistical~~data~~, and most analyses of road surface types

77 ~~are also based rely~~ on such statistics. For example, the International Road Federation
78 (IRF) provides statistical data related to road surface types, such as paved road length
79 and road paved rate (Turner, 2015; CIA, 2025). Greening et al. (2010) found, based on
80 IRF and other road statistics, that in Sub-Saharan Africa, the proportion of ~~"all-season~~
81 ~~road"roads"~~ (e.g., paved roads) does not exceed 30%. Kresnanto (2019) used statistical
82 data on paved road ~~length data lengths~~ from Badan Pusat Statistik Indonesia (BPS
83 Indonesia) to analyze the relationship between road paved rates and vehicle ownership
84 in Indonesia from 1957 to 2016. Patrick et al. (2022) conducted a survey to estimate
85 the road paved rate in rural areas of Sub-Saharan Africa. However, analyses of road
86 surface types based on statistical data have many limitations. On the one hand, existing
87 statistical data on road surface types do not cover all countries; for example, in 2020,
88 IRF ~~only~~ provided statistics on paved road lengths for only 19 African countries, and
89 some countries still face issues with untimely data updates (Barrington-Leigh et al.,
90 2017). On the other hand, these statistical data are collected indirectly by relevant
91 statistical departments or road authorities through surveys and ~~data~~ coordination of data
92 from various sources (Turner, 2015; CIA, 2025), making it ~~still~~ impossible to accurately
93 ~~identify determine~~ whether each road within a country or region is paved or unpaved.

94 In recent years, with the development of sensing devices, remote sensing, and big
95 data technologies, many ~~scholars~~researchers have proposed methods to identify road
96 surface types based on multiple data sources (Louhghalam et al., 2015; Sattar et al.,
97 2018; Pérez-Fortes et al., 2022). For example, some scholars have suggested methods
98 using vehicle-mounted sensing devices to identify road surface types. Chen et al. (2016)

设置了格式: 突出显示

99 designed a road surface type identification system that can be connected to distributed
100 vehicles and was tested on 100 taxis in Shenzhen to assess the roughness of road
101 surfaces in Shenzhen. Harikrishnan et al. (2017) collected vehicle speed data using the
102 XYZ three-axis accelerometer of smartphones and established road surface type
103 identification models for four different vehicle speeds. Li and Goldberg (2018)
104 developed a similar system using smartphones, collecting data from five different
105 drivers over 15 days to classify road roughness into three categories: "good", "
106 "moderate", and "
107 "poor". Other scholars have proposed methods using
108 street view data to identify road surface types. Randhawa et al. (2025) used a deep
109 learning model combining SWIN-Transformer and CLIP-based segmentation on
110 Mapillary street-view images to classify road surfaces ~~of global range~~ globally into
111 paved and unpaved. Menegazzo et al. (2020) collected street view data for some roads
112 in Anita Garibaldi, Brazil, using vehicle-mounted cameras and identified paved and
113 unpaved roads based on a CNN neural network model. Zhou et al. (2025a) recently
114 utilized crowdsourced street view data from Mapillary to develop a dataset of road
115 surface type annotations (paved and unpaved) for the African region. Additionally,
116 some scholars have proposed methods using high-resolution remote sensing imagery to
117 identify road surface types. Workman et al. (2023) developed a framework using high-
118 resolution optical satellite imagery and machine learning to predict the condition of
119 unpaved roads in Tanzania. Zhou et al. (2024) proposed a method that integrates
120 OpenStreetMap (OSM) and high-resolution Google satellite imagery to identify road
surface types and used this method to develop the road surface type dataset for Kenya.

设置了格式: 突出显示

设置了格式: 非突出显示

设置了格式: 字体: Times New Roman, 小四

121 However, methods based on vehicle-mounted sensing devices require on-site data
122 collection for each road, which inevitably requiringdemands significant manpower,
123 materialmaterials, and financial resources, making them difficult to apply to large-scale
124 study areas such as continents or countries. Data like Google street view are only
125 available only in a fewlimited number of countries or specific regions ofwithin
126 countries, making it challenging to identify the surface types of all roads in-a
127 countrynationwide. Therefore, although thedatadatasets developed based on street

128 views covers a global range, it only has 36% of the complete global roads, this
129 proportion is even lower in Africa and Asia (Randhawa et al., 2025). Remote sensing
130 methods may suffer from low accuracy in identifying road surface types due to dense
131 vegetation or building shadows obscuring roads (Zhou et al., 2024). Therefore, Zhou et
132 al. (2025b) recently proposed a new method based on multisource big data and deep
133 learning models to infer road surface types, which has been validated in two African
134 countries. Compared to remote sensing methods, this approach can address the low
135 accuracy of road surface type identification in areas with poor remote sensing image
136 quality; for example, the accuracy of remote sensing methods in Cameroon is only 67%,
137 while the accuracy ofwhereas the multisource data method achieves accuracy
138 exceeding 85% in the same regionexceeds 85%.

139 Nevertheless, existing research still has limitations. (1) The method proposed by
140 Zhou et al. (2025b) has only been validated in only a few (1-2) African countries, and
141 it remains to be verified whether these methods can be applied to develop road surface
142 type dataset for different African countries. (2) Existing road surface type data are still

143 mainly statistical data at the national scale, with Zhou et al. (2025b) only providing 2024)
144 provided a road surface type dataset only for NigeriaKenya, leaving a gap in data
145 products covering different other countries and regions in across Africa.

146 Therefore, this study aims not only aims to evaluate whether the universal
147 applicability of a method offor developing road surface type dataset based on
148 multisource big data and deep learning models has universal applicability but also
149 uses to apply this method to develop create the first dataset of road surface types (paved
150 and unpaved) for 50 countries and regions in Africa. The dataset developed in this study
151 not only provides information on the surface type of each road in various countries or
152 regions of Africa but also verifies the accuracy of the dataset: accuracy ranges from 77%
153 to 96%, and the F1 score ranges from 0.76 to 0.96. Compared to IRF and other road
154 statistical data, the dataset developed in this study can support detailed mapping of road
155 surface types in various African countries or regions and provide data support for road
156 infrastructure construction.

157 The remainder of this paper is organized as follows: Section 2 introduces describes
158 the study area and the source data used for developing and evaluating the road surface
159 type data. Section 3 introduces outlines the methods employed for data development
160 and evaluation. Section 4 reports presents the evaluation results of the road surface type
161 data. Section 5 discusses the implications and limitations of this the study. The last final
162 two sections provided detail the data acquisition methods and provide the research
163 conclusions.

164

165 **2. Study Area and Data**

166 **2.1 Study area**

167 This study takes 50 countries and regions in Africa, the second-largest continent on
168 Earth, as the study area (Figure 1), with a total road length of approximately 6,822,516
169 kilometers. ~~The main reason for selecting~~ Africa was selected as the study area ~~is~~
170 ~~that primarily because~~ existing research ~~shows that the indicates a high~~ proportion of
171 unpaved roads ~~in Africa is high across the continent~~ (Biber-Freudenberger et al., 2025),
172 ~~while~~. However, the IRF only provides statistics on ~~the length of paved roads road~~
173 ~~lengths~~ and ~~the road paved rate paving rates~~ for some African countries. Due to the lack
174 of ~~spatialized a spatially detailed~~ road surface type dataset, it is ~~difficult challenging~~ to
175 ~~provide offer~~ decision support for improving road infrastructure in Africa.

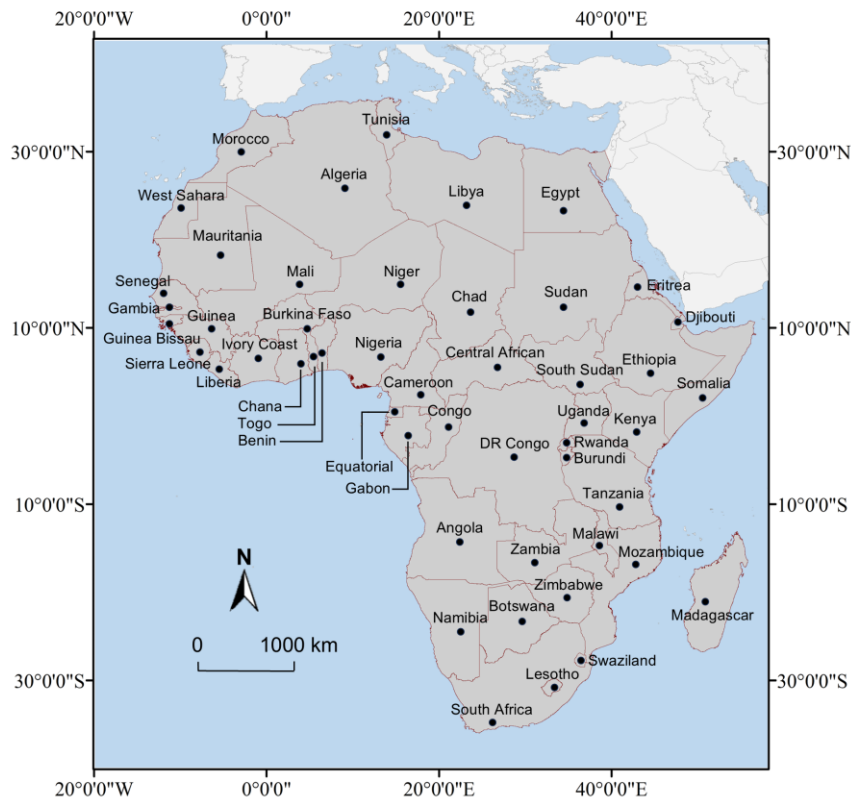


Figure 1. Study ~~area~~Area

176

177

178

179 2.2 Data

180 2.2.1 Geospatial data

181 (1) OpenStreetMap road data: OpenStreetMap (OSM) is an open geospatial dataset

设置了格式: 字体: +西文正文(等线), 五号

182 ~~provided online contributed~~ by global volunteers and made available online

183 (Harikrishnan et al., 2017). This dataset includes various geographic elements such as

184 roads, buildings, and water bodies. Each geographic element not only contains

185 geometric information but also describes its characteristics or attribute information

186 through a series of tags. Specifically, the “surface” tag in OSM road data is designed
187 to describe the road surface type of each road segment. The value of this tag typically
188 refers to the surface material of the road, such as asphalt, concrete, or gravel. **Although**
189 OSM data for different countries or regions in Africa ~~all~~ include **information on road**
190 **surface type information** ~~types~~, incomplete statistics show that the length of OSM roads
191 with surface type information in a single country usually accounts for less than 30%,
192 meaning that most OSM road data lack surface type information, ~~thus urgently~~
193 ~~requiring highlighting an urgent need for~~ supplementation and improvement. This study
194 obtained road data for 50 countries and regions in Africa (in ESRI Shapefile format)
195 from the Geofabrik platform (<http://download.geofabrik.de/index.html>), which allows
196 obtaining OSM road data by country.

197 (2) GDP grid data: This dataset is a 1km spatial resolution GDP grid dataset developed
198 by Southwestern University of Finance and Economics (Chen et al., 2022). The dataset
199 was developed by integrating nighttime light remote sensing data (NPP-VIIRS), land
200 use data, and regional economic statistics using spatial interpolation and machine
201 learning algorithms. This dataset overcomes the limitations of traditional administrative
202 unit statistics and ~~can precisely depict~~accurately captures the spatial heterogeneity of
203 economic activities. The dataset ~~spans~~covers the period from 1992 to 2019, ~~and~~ this
204 study ~~used the utilized~~ data from the most recent year (2019).

205 (3) Population grid data: This dataset is the LandScan global population dataset
206 developed by Oak Ridge National Laboratory (ORNL) in the United States, with a
207 spatial resolution of 30 arc seconds in latitude and longitude (approximately 1km at the

设置了格式: 突出显示

设置了格式: 突出显示

设置了格式: 突出显示

设置了格式: 突出显示

设置了格式: 突出显示

设置了格式: 字体: (默认) 宋体, 连字: 无

208 equator) (Dobson et al., 2000). The dataset integrates census data, satellite imagery, and
209 mobile communication data, using dynamic modeling methods to simulate 24-hour
210 population distribution. Existing research has found that compared to other population
211 grid datasets (such as WorldPop and Global Human Settlement Population Grid),
212 LandScan has higher accuracy (Jiang et al., 2021; Mohit et al., 2021; Yin et al., 2021).
213 Therefore, this study obtained the 2020 LandScan population raster data for the African
214 region (<https://landscan.ornl.gov/>).

215 (4) Building height data: This dataset ~~is provides building height information at~~ a 100-
216 meter resolution ~~building height dataset and is~~ released by the Global Human Settlement
217 Layer (GHSL). The dataset is based on Sentinel-1/2 and Landsat imagery, using
218 machine learning algorithms to extract the three-dimensional morphology of buildings
219 (Pesaresi et al., 2021). The dataset includes ~~building height~~-raster data ~~representing~~
220 [building heights](#). GHSL-BUILT is the world's first building height dataset, and this
221 study obtained the 2018 building height data recommended by GHSL for analysis
222 (https://human-settlement.emergency.copernicus.eu/ghs_buH2023.php).

223 (5) Land cover data: This dataset is a global land cover dataset with a 10-meter spatial
224 resolution released by ESRI. The dataset was developed based on Sentinel-2 imagery
225 and deep learning methods, including nine different land cover categories (water, trees,
226 flooded vegetation, crops, buildings, bare land, snow, clouds, and pasture) (Karra et al.,
227 2021). Existing research indicates that ESRI land cover data ~~has better exhibits higher~~
228 accuracy compared to other similar datasets (such as ESA World Cover and Dynamic
229 World) (Yan et al., 2023). This study obtained the 2020 Land Cover data for the African

230 region (<https://livingatlas.arcgis.com/landcover/>).

231 **2.2.2 Statistical data**

232 To verify the effectiveness of the data, this study also ~~obtained collected~~ two types of
233 statistical data, IRF road statistics and socio-economic statistics. 带格式的: 缩进: 首行缩进: 0 厘米

234 (1) IRF Road Statistics: The International Road Federation (IRF) is a non-profit
235 international organization dedicated to promoting development and cooperation in the
236 global road transport sector (Turner, 2015). IRF provides free ~~and rich, comprehensive~~
237 statistical data resources to ~~global~~ users worldwide (<https://www.irf.global/>). These data
238 primarily come from authoritative reports and statistical agencies of various
239 governments, covering multiple fields such as road networks and the transportation
240 industry. This study ~~obtained utilized~~ three statistical data provided by IRF for the
241 African region in 2020, ~~namely:~~ the length of paved roads, total road length, and road
242 paved rate.

243 (2) Socioeconomic Statistics: Existing research has found that the road paved rate is
244 ~~highly~~strongly positively correlated with the level of socioeconomic development
245 (Anyanwu et al., 2009). Therefore, this study also introduced two indicators related to
246 the level of socioeconomic development, namely the Human Development Index (HDI)
247 and Gross National Income per capita (GNI per capita, based on PPP current
248 international \$). HDI ~~is~~, compiled and published by the United Nations Development
249 Programme since 1990, ~~obtained by comprehensively evaluating is derived from a~~
250 comprehensive evaluation of a country's life expectancy, average years of schooling,
251 and gross national income, and is used to measure the socioeconomic development level

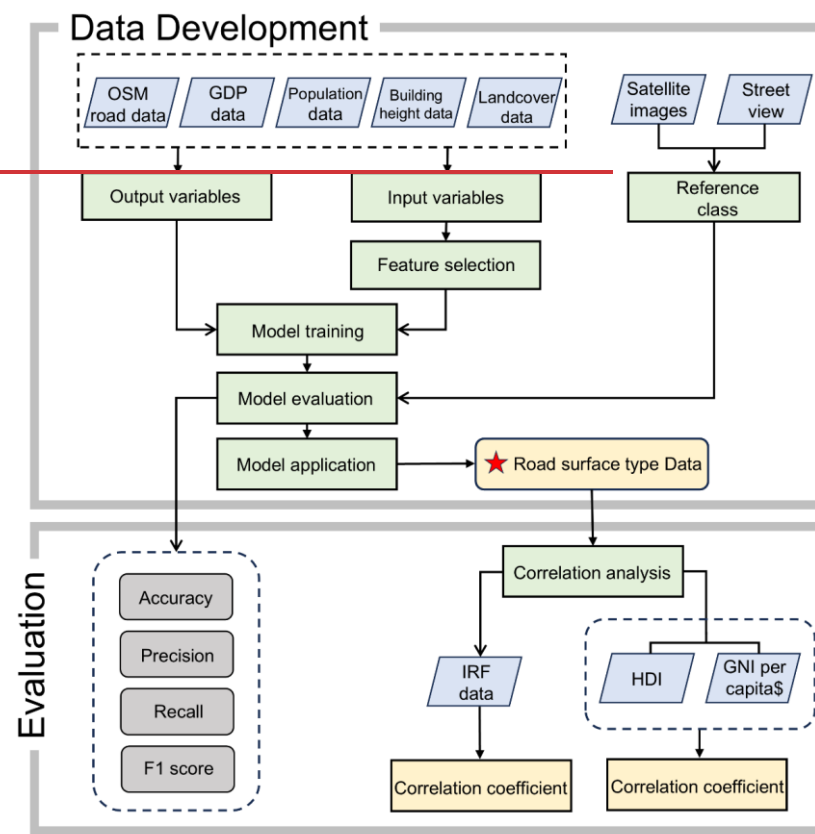
设置了格式: 字体: 小四

252 of various countries. GNI per capita is published by the World Bank, where GNI is the
253 sum of the incomes of all residents in a country or region; GNI per capita is the average
254 GNI of a country or region, which can measure the average economic income level of
255 the nationals in a country or region. This study obtained ~~the~~ 2020 HDI and GNI per
256 capita data, covering 44 and 36 African countries and regions, respectively.

257

258 **3. Methods**

259 The technical roadmap of this study is shown in Figure 2.



260

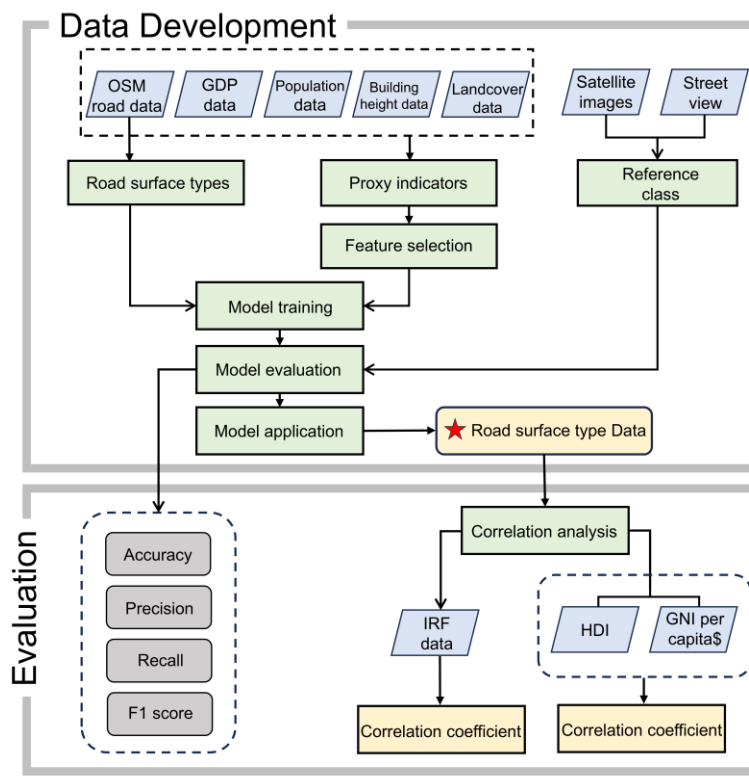


Figure 2. Technical ~~roadmap~~Roadmap

3.1 Developing of Road Surface Type Dataset of Africa

This study utilizes a method recently proposed by Zhou et al. (2025b) ~~that is based on~~, which leverages multi-source geospatial big data and deep learning models to develop the road surface type dataset ~~offer~~ 50 African countries and regions. The main idea of this method ~~includes~~involves the following steps: First, sampling points and ~~their~~ corresponding OpenStreetMap (OSM) road surface type labels are acquired based on OSM road data. ~~Then~~Next, proxy indicators that characterize road surface types are calculated based on multi-source open geospatial big data. Third, a deep learning model

272 is trained using ~~the~~these proxy indicators and road surface type labels of the sampling
273 points. Finally, the trained model is applied to the road networks of various African
274 countries and regions to identify the surface type of each road.

275 **3.1.1 Road Sampling**

276 According to the definition of OSM road level tags (highway=) ~~as~~ outlined in the OSM
277 wiki (<https://wiki.openstreetmap.org/wiki/Key:highway>), roads passable by four-
278 wheeled motor vehicles are selected. These specifically include: “highway= motorway,
279 motorway_link, trunk, trunk_link, primary, primary_link, secondary, secondary_link,
280 tertiary, tertiary_link, residential, living_street, service, track, road, unclassified”. Other
281 roads primarily intended for bicycles or pedestrians (e.g., cycleway, footway) are
282 excluded from the analysis.

283 ~~After that~~Afterward, the selected OSM road data are ~~then~~ sampled at 100-meter
284 intervals to generate sampling points. The 100-meter interval is chosen because most
285 roads are greater than or equal to 100 meters in length, ensuring that most roads have
286 at least one sampling point. For roads shorter than 100 meters, the ~~center point~~midpoint
287 of the road is used as the sampling point.

288 **3.1.2 Calculation and Selection of Proxy Indicators**

289 (1) Calculation of Proxy Indicators

290 It has been found by Zhou et al. (2025b) that road surface types are not only related to
291 road classes but also to the socio-economic and geographical environment of the area
292 where the road is located. Therefore, Zhou et al. (2025b) designed 16 proxy indicators
293 across three feature dimensions—Road network features, Socio-economic features, and

294 Geographical environment features—as shown in Table 1. These indicators serve as

295 “proxies” to identify or infer road surface types.—

296

设置了格式: 突出显示

设置了格式: 突出显示

297

带格式的: 两端对齐, 缩进: 首行缩进: 0.74 厘米, 行距: 2 倍行距, 无孤行控制

298

Table 1. Proxy Indicators

Dimension	Data Source	No.	Input	Type
Road network features	OSM road data	1	Road class	Category
		2	Road length	Value
		3	Degree	
		4	Closeness	
		5	Betweenness	
Socio-economic features	GDP	6	GDP	Value
	Population	7	Population	
	Building height	8	Building height	
Geographical environment features	Land cover	9	Water proportion	Value
		10	Trees proportion	
		11	Flooded vegetation proportion	
		12	Crops proportion	
		13	Building proportion	
		14	Bare land proportion	
		15	Snow land proportion	
		16	Pasture proportion	

299

300

For a single road sampling point:

301

Road network features: The road class is directly obtained from the OSM

302

"highway=" tag. To calculate road length, degree centrality (Degree), closeness

设置了格式: 突出显示

303

centrality (Closeness), and betweenness centrality (Betweenness). The road

设置了格式: 突出显示

304

networks of each country or region are constructed into strokes based on the "every

设置了格式: 突出显示

305 best fit" method (Zhou et al., 2012). "rule. The core principle of this method is to
306 connect continuous road segments into individual roads (called "strokes"), according
307 to the deflection angle between adjacent road segments. These metrics (road length,
308 Degree, Closeness, Betweenness) are calculated for each stroke. The, by referring to
309 Zhou and Li (2015); Zhou et al. (2025b). Finally, the values are assigned to the
310 corresponding sampling points on the road. (Zhou et al., 2012).

设置了格式: 突出显示

311 Socio-economic features: The sampling point is assigned the value of the grid cell
312 it falls into for corresponding data (GDP, population, or building height).

313 Geographical environment features: A 100m x 100m grid unit is established. The
314 sampling point's grid unit is identified. The proportion of each land cover type within
315 that grid unit is calculated.

316 (2) Feature Selection

317 Since proxy indicators may be highly correlated, this study employs correlation
318 analysis and contribution analysis to select appropriate proxy indicators for
319 model training, aiming to reduce data dimensionality, simplify model complexity, and
320 eliminate multicollinearity.

321 For a single country or region: First, the correlation between pairs of proxy
322 indicators is calculated using Phi_k (Baak et al., 2020), chosen because it can measure
323 the correlation coefficient between different types of variables. Second, Shapley
324 Additive exPlanations (SHAP) are used to analyze the interpretability of each proxy
325 indicator, quantifying its contribution to the model's predictions. Third, proxy
326 indicators without multicollinearity are directly used as input features. If two proxy

327 indicators exhibit multicollinearity, the one with the highest contribution (based on
328 SHAP values) is retained as the input feature for that country or region. [In this study,](#)
329 [the selected proxy indicators for 50 African countries can be found in Appendix A.](#)

设置了格式: 突出显示

330 (3) Road surface type classification

331 Road surface types [from OSM data](#) are treated as output variables and defined into
332 two categories based on whether the road is paved. Paved roads: roads with a structured
333 surface. Unpaved roads: roads without a structured surface.

设置了格式: 突出显示

设置了格式: 突出显示

334 Since the labels for training samples are automatically extracted from the OSM
335 “surface=” tag, all OSM tags are reclassified into [“paved”](#) or [“unpaved”](#) roads, as
336 shown in Table 2. The reclassification criteria follow the guidelines provided by OSM’s
337 wiki (<https://wiki.openstreetmap.org/wiki/Surface>).

338 Table 2. Reclassifying OSM “surface=” [tags](#) into [paved](#) and [unpaved](#)
339 [roads](#)

OSM “surface=” Tag	Reclassification
Asphalt, Concrete, Concrete: Plates, Paved, Paving Stones, Sett	Paved
Compacted, Dirt, Earth, Fine_Gravel, Gravel, Ground, Mud, Pebblestone, Sand, Unpaved	Unpaved

340

341 3.1.3 Model Training and Application

342 Zhou et al. (2025b) compared six machine learning and deep learning models for

带格式的: 缩进: 首行缩进: 0 厘米

343 identifying road surface types and found that the TabNet model achieved the highest
344 accuracy (approximately 86%). Consequently, this study adopts TabNet to develop the
345 road surface type dataset for 50 African countries and regions. TabNet, proposed by
346 Arik et al. (2021), combines the end-to-end learning and representation learning
347 characteristics of deep neural networks (DNNs) with the interpretability and sparse
348 feature selection advantages of decision tree models.

349 For a single African country: From sampling points with “surface=” tags,
350 5,000 paved and 5,000 unpaved sampling points are randomly selected as
351 training samples. In for two reasons: Firstly, the positive and negative samples are
352 controlled at a 1:1 ratio to achieve equal weights, ensuring sufficient learning for both
353 types. Secondly, we found that the model's accuracy improves as the number of
354 sampling points increases, although it tends to stabilize once the sample size reaches
355 approximately 3,000 points. Despite of this, in some countries or regions where the
356 number of paved sampling points is less than 5000 (e.g., a minimum of approximately
357 3000), all paved sampling points (e.g., 3000) and an equal number of unpaved sampling
358 points (e.g., 3000) are used.

359 For each training sample, the 16 proxy indicators from Table 1 are calculated. After
360 feature selection, the selected proxy indicators serve as input features for model training.
361 The OSM road surface type of the training sample is used as the model output. The
362 TabNet model is trained, with parameters (e.g., learning rate, batch size, number of steps,
363 training epoch) automatically determined using the Optuna framework, which searches
364 for optimal parameters during training. The core principle of the Optuna framework is

设置了格式: 突出显示

设置了格式: 突出显示

设置了格式: 突出显示

设置了格式: 突出显示

设置了格式: 突出显示

设置了格式: 突出显示

365 to explore various parameter combinations until it identifies the one that yields the
366 highest accuracy. In this study, the search ranges for the parameters—learning rate,
367 number of steps and training epochs—were set to 0.001-0.2, 3-10, and 10-100,
368 respectively.

369 Each country trains a separate model. The trained model ~~infers~~predicts the road
370 surface type of each sampling point ~~in~~within that country. A correction strategy
371 proposed by Zhou et al. (2025b) is applied to determine the final surface type of each
372 road segment, where the surface type is determined by the majority surface type of its
373 sampling points.

374

375 **3.2 Result evaluation**

376 This study evaluates the effectiveness of the developed road surface type dataset from
377 three aspects.

378 **3.2.1 Accuracy assessment**

379 For each African country or region: From all sampling points (excluding training
380 samples), 500 points predicted as "paved" and 500 predicted as "unpaved" are
381 randomly selected, totaling 1000 validation points. Three different operators visually
382 interpret the classification results ~~off~~for each validation point using high-resolution
383 Google satellite imagery and Google street view, with the final reference surface type
384 is determined by voting.

385 ~~At last~~Finally, the model's predictions are compared with the reference road surface
386 types, and its effectiveness is assessed by calculating accuracy, precision, recall, and F1

387 score.

388 **3.2.2 Comparative evaluation with existing statistical data**

389 Based on the developed road surface type dataset, the paved road length, total road
390 length, and road paved rate for each country and region are calculated and compared
391 with International Road Federation (IRF) statistical data. Specifically, correlation
392 coefficients between the results calculated from this data product and IRF statistical
393 values are explored.

394 Since IRF provided statistical values for only 19 African countries in 2020, only
395 these 19 countries are included in the correlation analysis.

396 **3.2.3 Correlation evaluation with socio-economic indicators**

397 Existing research indicates that the road paved rate is highlystrongly positively
398 correlated with socio-economic development levels (Anyanwu et al., 2009). Therefore,
399 this study explores the correlation between the road paved rate calculated from this data
400 product and two indicators: Human Development Index (HDI), Gross National Income
401 per capita (GNI per capita, based on PPP current international \$).

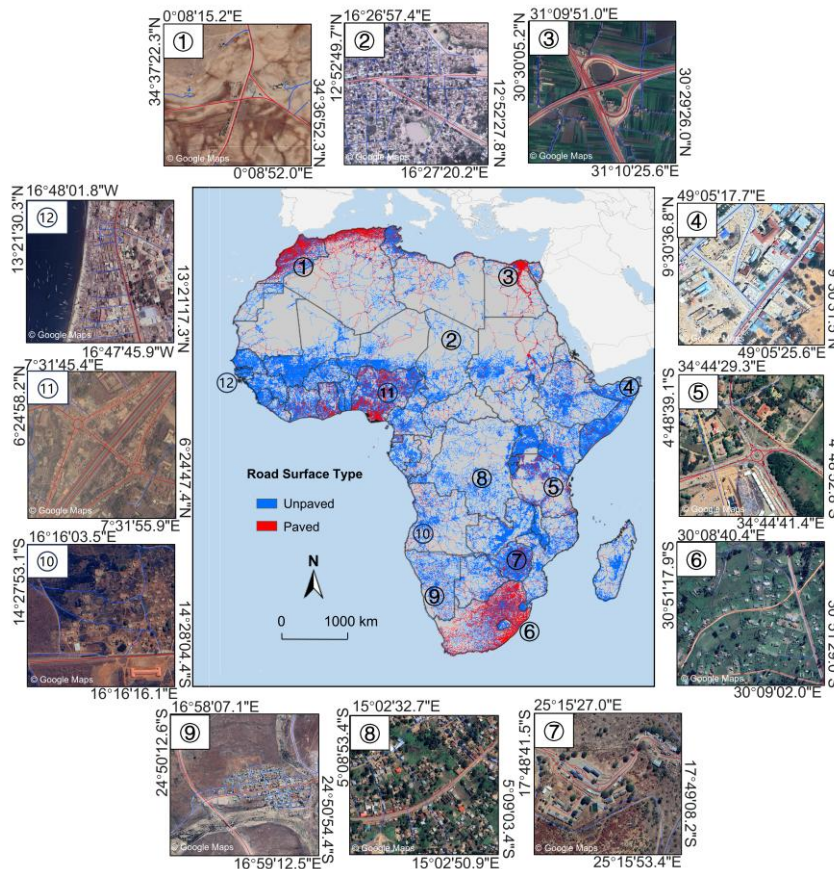
402 More precisely, the analysis includes 44 African countries with HDI data and 36
403 countries with GNI per capita statistical data to verify the effectiveness of the data
404 product.

405 406 **4. Results and Analyses**

407 **4.1 Description of the Africa Road Surface Type Dataset**

408 This study has developed the road surface type dataset that records the roads and its
带格式的: 缩进: 首行缩进: 0 厘米

409 surface type attribute information for 50 African countries and regions, as shown in
410 Figure 3.



411
412 Figure 3. Visualization of [road surface type dataset for Road Surface Type Dataset For](#)

413 50 African [countries](#)[Countries](#) and [regions](#)[Regions](#) (source: Google Maps. 2025,

414 <https://www.google.com/maps/> (last access: 2 Jul 2025))

415 This dataset was developed based on OpenStreetMap (OSM) road data for

设置了格式: 突出显示
带格式的: 缩进: 首行缩进: 2 字符

416 Africa, with each country and region stored as a separate vector file in ESRI Shapefile

417 format, using the WGS 1984 Web Mercator projection. The road data for each country

418 and region includes include five attribute fields: road ID, coordinates of the start and
419 end points (see Table 3), road length, and road surface type. The entire dataset
420 comprises approximately 13,309,000 road segments, with a total length of about
421 6,822,516 km.

设置了格式: 突出显示

设置了格式: 突出显示

422 Table 3. Descriptions of dataset

Attribute	Description	Type
ID	Road segment ID	Int
Start point	Coordinates of the road segment's start point (x, y)	String
End point	Coordinates of the road segment's end point (x, y)	String
Road length	Length of the road segment (calculated based on WGS 1984 Web Mercator)	Float
Surface type	Road surface type, i.e., paved or unpaved	String

设置了格式: 突出显示

设置了格式: 突出显示

设置了格式: 突出显示

设置了格式: 突出显示

设置了格式: 突出显示

423

424 4.2 Accuracy Assessment of the Road Surface Type Identification Model

425 The accuracy assessment results for the road surface type dataset foracross 50 African
426 countries and regions are presented in Figure 4. As indicatedshown in the figure, the
427 average accuracy across the 50 countries and regions is 86.8%. Out of these, 44
428 countries and regions have an accuracy above 80%, and 12 out of 50 have an accuracy
429 exceeding 90%. The country with the highest accuracy is Burundi, surpassing 96%,
430 while the lowest is Egypt, at approximately 77%.

431 For paved roads, the average precision, recall, and F1 score across the 50 countries
432 and regions are 88.0%, 85.0%, and 0.86, respectively. Specifically, 45 countries and

带格式的: 缩进: 首行缩进: 0 厘米

433 regions have a precision above 80%, 32 have a recall above 80%, and 43 have an F1
434 score above 0.80 for paved roads.—

435 For unpaved roads, the average precision, recall, and F1 score are 86.3%, 88.2%,
436 and 0.87, respectively. Among the 50 countries and regions, 36 have a precision above
437 80%, 46 have a recall above 80%, and 46 have an F1 score above 0.80 for unpaved
438 roads.—

439 These results demonstrate that the road surface type dataset developed in this study
440 has relatively high accuracy, consistent with the accuracy reported in existing research
441 (approximately 86%) (Zhou et al., 2025b), indicating that the method using multi-
442 source geospatial big data and deep learning models for identifying road surface types
443 has certain universalitya degree of generalizability.

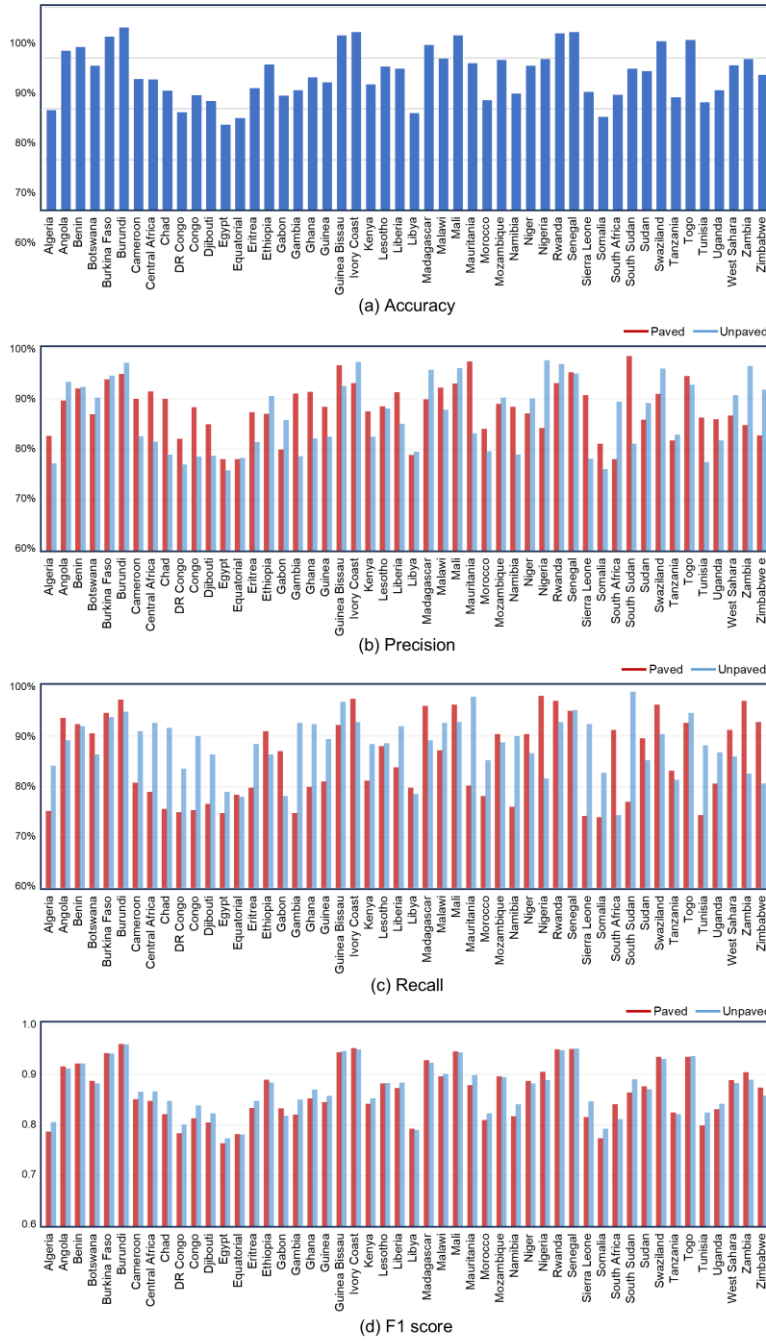


Figure 4. Accuracy Assessment Results of the Road Surface Type Dataset

446

447 **4.3 Comparative Assessment with IRF Statistical Data**

448 Figure 5 presents the correlation analysis results between the total road length, paved
449 road length, and road paved rate calculated based on the road surface type dataset
450 developed in this study, and the corresponding statistical data from the International
451 Road Federation (IRF).

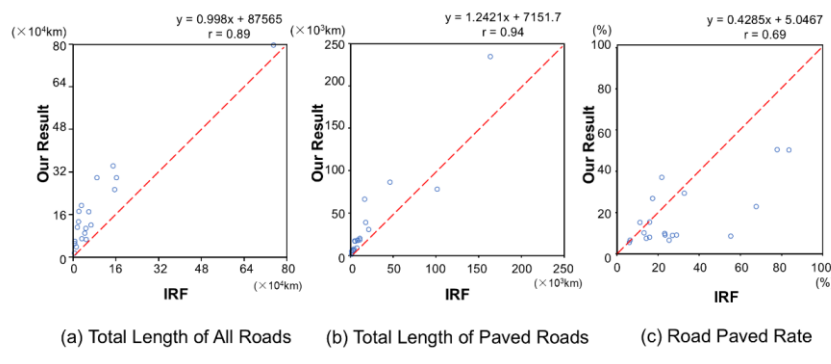
452 The correlation coefficients for total road length, paved road length, and road paved
453 rate are 0.89, 0.94, and 0.69, respectively, all indicating ~~a high correlation, strong~~
454 ~~correlations~~. This suggests that the calculations based on our data product are generally
455 consistent with the IRF statistical data in terms of trends. For example, South Africa
456 has the longest total ~~road length~~ and paved road ~~length~~lengths, while Gambia has the
457 shortest; Tunisia and Morocco have the highest road paved rates. These results indicate
458 the ~~rationality~~validity of the road surface type dataset.

459 However, as shown in the scatter plots (Figure 5), ~~there are still~~ discrepancies
460 ~~remain~~ between the calculations based on our data product and the IRF statistical data.
461 Specifically, the total road length calculated from our data product is consistently higher
462 than that reported by IRF (as seen in Figure 5a, where points are located to the left of
463 the diagonal). Similarly, for 18 out of 19 countries, the paved road length is higher than
464 the IRF statistics. Existing research has pointed out that IRF statistical data may
465 underestimate ~~the~~ total road length globally, with an average underestimation of 36%,
466 and for 94 countries, the underestimation exceeds 50% (Barrington-Leigh et al., 2017).
467 Therefore, IRF statistical data may underestimate ~~the~~both total ~~road length~~ and paved

带格式的: 缩进: 首行缩进: 0 厘米

468 road lengthlengths in African countries.

469 Additionally, ~~for~~in 15 out of 19 countries, the road paved rate is lower than that
470 reported by IRF. This may be because IRF data underestimates the total road length in
471 African countries, and the unaccounted roads are likely mostly unpaved, leading to an
472 overestimation of the road paved rate in IRF statistics.



473
474 Figure 5. The Correlation Analysis Results with IRF Statistical Data

475

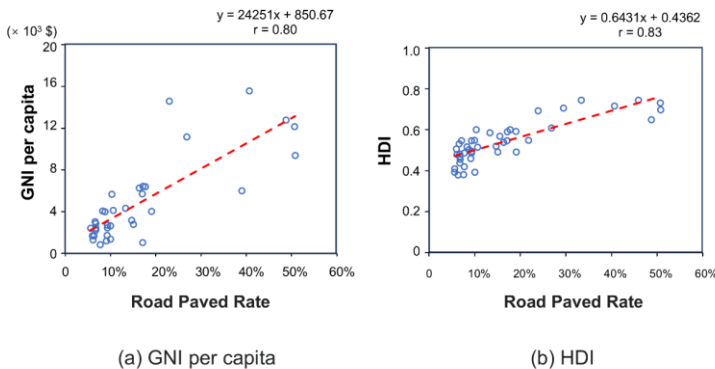
476 4.4 Correlation Assessment with Socioeconomic Indicators

477 The correlation analysis results between the road paved rate calculated based on our
478 data product for 50 African countries and regions and both the Gross National Income
479 per capita (GNI per capita) and the Human Development Index (HDI) are shown in
480 Figure 6. As indicatedshown, the correlation coefficients between the road paved rate
481 and GNI per capita and HDI are 0.80 and 0.83, respectively, both showingindicating a
482 strong positive correlation in both cases. This indicatessuggests that the road paved
483 rate in African countries is highly positively correlatedassociated with their level of
484 socioeconomic development, consistent with findings from existing research

带格式的: 缩进: 首行缩进: 0 厘米

485 (Anyanwu et al., 2009), indirectly validating the effectiveness of our road surface type

486 dataset.



487

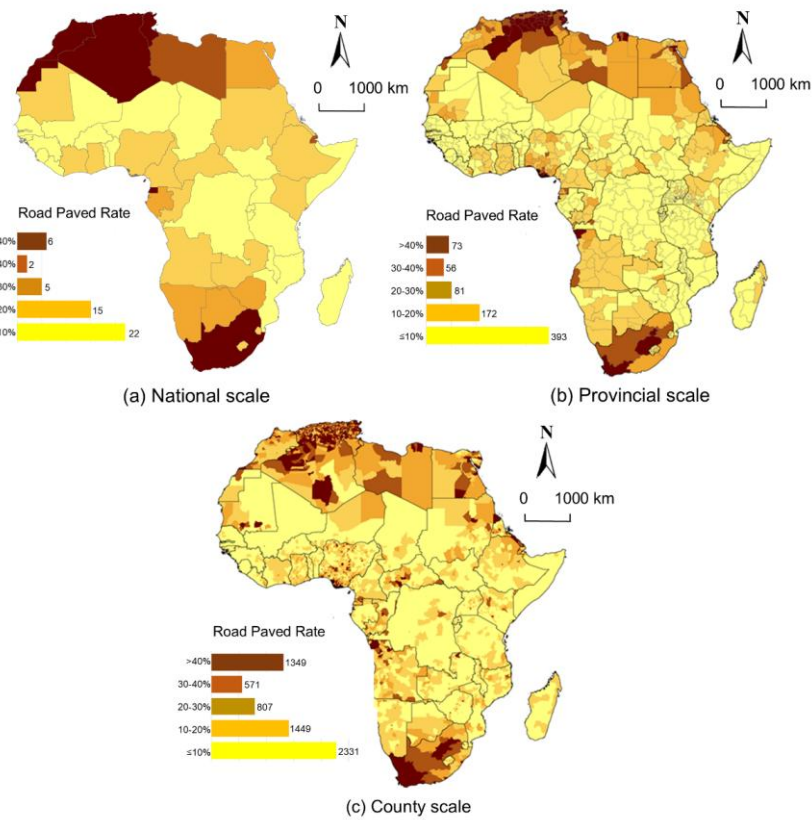
488 Figure 6. The Correlation Analysis Results of ~~The~~ Road Paved Rate Calculated Based
489 on ~~The~~ African Road surface type dataset with Per Capita GNI (a) and HDI (b)

490

491 4.5 Spatial Pattern Analysis of Road Paved Rates in Africa

492 Based on the road surface type dataset, the spatial patterns of road paved rates in 50
493 African countries and regions were analyzed at the national, provincial, and county
494 levels, as shown in Figure 7. Compared to IRF, which only provides statistical data for
495 19 African countries (Ken et al., 2008), our dataset not only allows for the analysis of
496 road paved rates in all 50 African countries and regions but also enables detailed
497 analysis at different administrative levels.

带格式的: 缩进: 首行缩进: 0 厘米



498
499 Figure 7. Spatial Pattern Analysis at the National, Provincial, and County Levels
500

501 At the national level, the average road paved rate across the 50 African countries
502 and regions is only 17.4%, ranging from a low of 5.54% in Chad to a high of 50.77%
503 in Morocco. Only six African countries have a road paved rate above 40%, while 37
504 countries and regions have a-rates below 20%. The average road paved rate for 43
505 countries and regions in Sub-Saharan Africa (excluding South Africa) is merely 13.6%.
506 These results indicate that road paved rates in African countries and regions are
507 generally low, with significant north-south disparities. At the provincial and county

508 levels, only 9% of provincial administrative divisions have a road paved rate above
509 40%, mostly located in north of North Africa and South Africa. Similarly, only about
510 20% of county administrative divisions have a road paved rate above 40%, primarily in
511 north of North Africa, South Africa, and some urban areas. Therefore, the overall spatial
512 pattern of road paved rates in Africa shows a “higher in the north and south, lower in
513 the central region” distribution, with higher rates in north of North Africa and South
514 Africa, and lower rates in Sub-Saharan Africa excluding South Africa. The average road
515 paved rate in the north of North Africa (40.7%) is approximately three times that of Sub-
516 Saharan Africa (excluding South Africa).

517

518 **5. Discussion**

519 **5.1 Data Quality**

520 This study developedThis study employed multi-source geospatial data and deep
521 learning model to develop road surface type dataset for 50 African countries and regions
522 and verified its validity (accuracy ranging from 77% to 96%; F1 score ranging from
523 0.76 to 0.96). However, the quality of the dataset varies across different African
524 countries and regions. For example, Burundi has an accuracy of 96%, while Egypt's
525 accuracy is only 77%. This is likely because the proposed approach relies heavily on
526 the proxy indicator “Road class” (Appendix A), and thus the proportions of various
527 road classes may influence the quality of the developed dataset.
528 In order to verify this, Figure 8 shows the classification accuracies for nine main
529 road classes in the 50 African countries. For each country and each road class, 100

设置了格式: 字体: (默认) 宋体, 连字: 无

530 sampling points were randomly selected for analysis. As shown, most classification
531 accuracies for these road classes are close to or exceed 80%, with some classes—
532 specifically “Motorway”, “Trunk” and “Primary”—achieving accuracies above 95%.
533 These results demonstrate the effectiveness of the road surface type dataset, which is
534 consistent with the finding in Figure 4. However, the classification accuracies for the
535 four road classes—“Residential”, “Service”, “Track” and “Unclassified”—are
536 generally lower than those of other road classes. This is probably because high-class
537 roads are predominantly paved and can be easily identified; in contrast, low-class roads
538 may consist of a mix of paved and unpaved surfaces, making road surface classification
539 more difficult. Moreover, Figure 9 plots the relationship between the proportions of
540 “Residential”, “Service”, “Track” and “Unclassified” roads in 50 African countries and
541 the surface type classification accuracies for these countries. This figure shows that the
542 proportions of both “Residential” and “Service” roads have a moderate negative
543 correlation (i.e., -0.405 and -0.527, respectively) with the corresponding classification
544 accuracy of each country. This finding confirms that the proportions of certain road
545 classes (e.g., “Residential” and “Service”) may affect the quality of the road surface
546 type dataset. For instance, the higher the proportion of “Residential” roads (e.g., 78%
547 for Egypt), the lower the corresponding classification accuracy (e.g., 77% for Egypt).
548

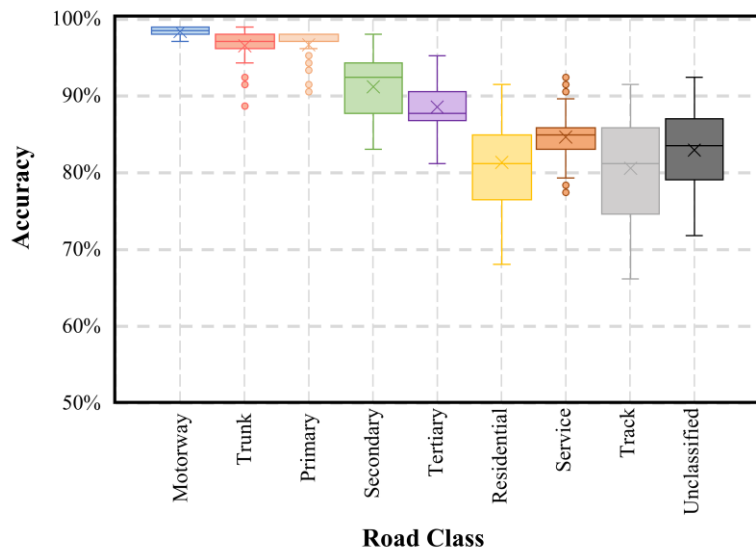
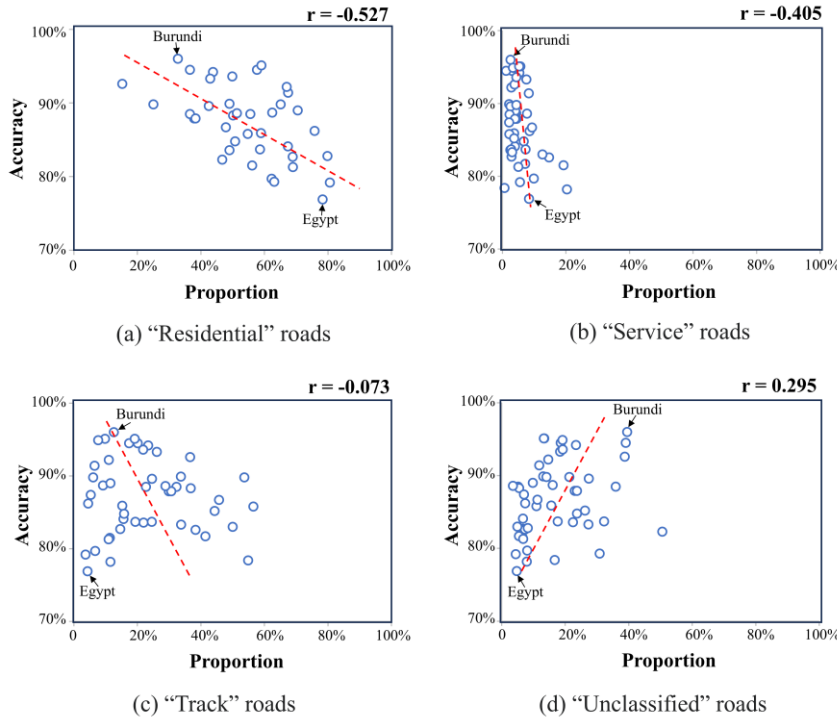


Figure 8. The Box Plot to Show the Classification Accuracy for Each of Main Road

Classes For 50 African Countries.

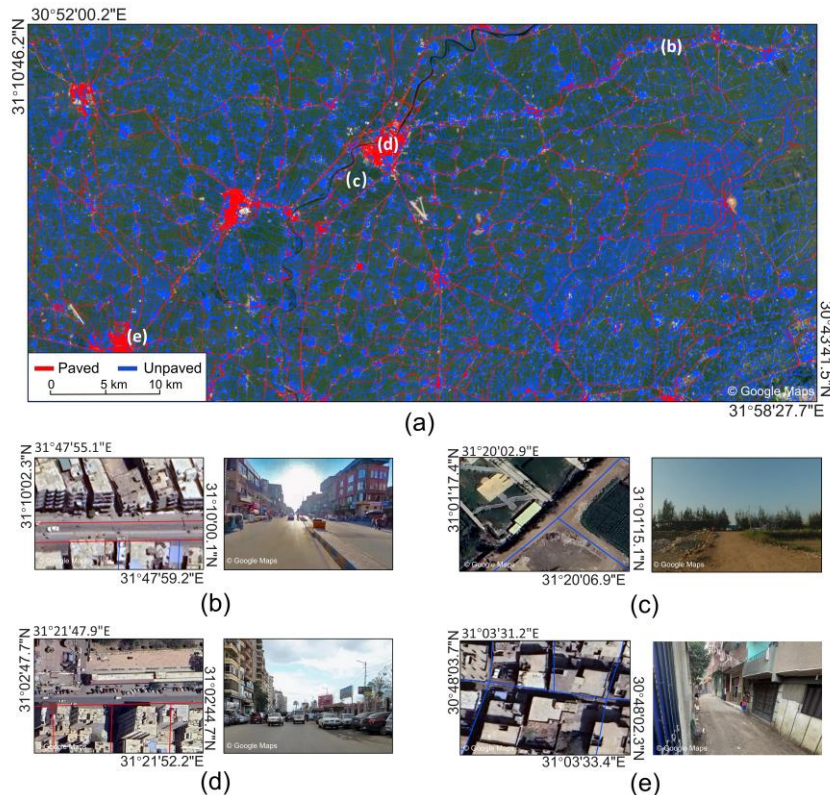


553 **Figure 9. The Correlation Between the Proportions of Four Road Classes (a.**

554 **“Residential”**, b. **“Service”**, c. **“Track”** And d. **“Unclassified”**) and Corresponding

555 **Classification Accuracies For 50 African Countries.**

556 Further, taking a local area in Egypt as an example, combined with Google high-
 557 resolution remote sensing imagery and Google street view, it can be observed that the
 558 backbone of the road network in this region predominantly consists of paved roads
 559 (Figure 8b_10b), while non-backbone roads (especially in rural areas) are mostly
 560 unpaved (Figure 8e_10c); urban areas in Egypt are predominantly paved (Figure 8d_10d),
 561 although some roads remain unpaved (Figure 8e_10e). These results indicate that the
 562 road surface type classification in this study is reasonable.
 563



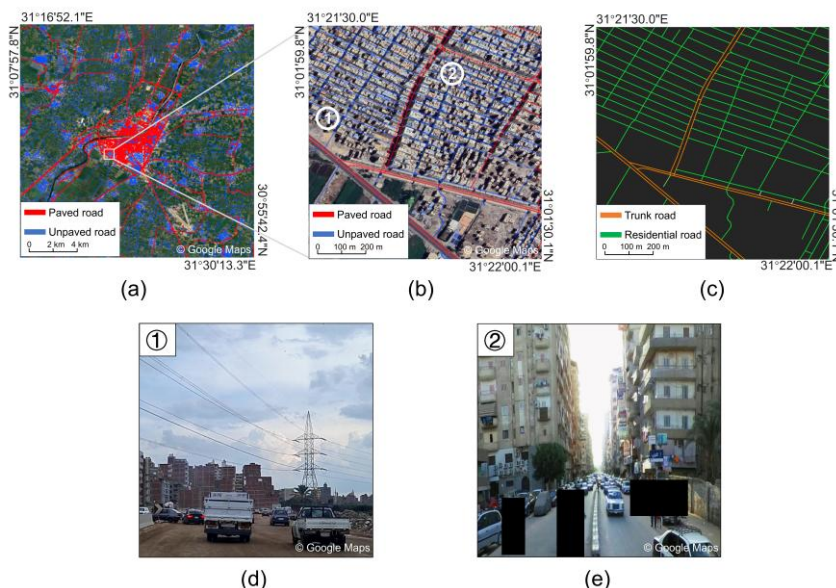
564
565 Figure 8.10. An Example of Road Surface Type ~~Data~~Dataset in Egypt (source: Google
566 Maps. 2025, <https://www.google.com/maps/> (last access: 2 Jul 2025))

567
568 Despite this, ~~we found that~~ misclassifications of road surface types are inevitable.

569 Taking urban areas in Egypt as an example (Figure 9a~~11~~a), Figure 9b~~11~~b shows a 1 km
570 \times 1 km grid area in this region. Figure 9e~~11~~c displays two road classes ~~in~~within this
571 grid area: ~~"trunk"~~ and ~~"residential"~~. From Figures 9b~~11~~b and 9e~~11~~c, it ~~can be~~
572 ~~seen~~is evident that most "trunk" roads in this area are classified as paved, while most
573 "residential" roads are classified as unpaved. However, ~~based on~~ street view imagery ~~of~~
574 ~~this area, it is evident~~reveals that "residential" roads include both unpaved (Figure

575 ~~9d11d~~ and paved (Figure ~~9e11e~~) types. Therefore, ~~it is difficult to~~
576 ~~distinguish~~₂ ~~distinguishing~~ road surface types in this area based solely on road class, ~~and~~
577 ~~is difficult. Additionally,~~ the spatial resolution of the GDP and population data we
578 obtained (both 1 km) also makes it challenging to finely differentiate road surface types
579 within this area.

设置了格式: 字体: 小四



580
581 Figure 911. An Example of Explaining the Data Quality of ~~The~~ the African Road

582 ~~surface type dataset~~ Surface Type Dataset (source: Google Maps. 2025,

583 <https://www.google.com/maps/> (last access: 2 Jul 2025))

584 Additionally, open geospatial data inevitably have quality issues. For instance,
585 although existing studies have found that the geometric positional accuracy and
586 completeness of OSM road data in Africa are generally high, ~~gaps in~~ road data ~~gaps~~ are
587 unavoidable (Zhou et al., 2022); road surface types and road classes labeled by global
588 volunteers in OSM may also contain errors (Zhou et al., 2022). The GHSL-BUILT

589 building height data, derived from medium-resolution remote sensing imagery
590 (Sentinel-2), also inevitably has estimation biases for building heights (Pesaresi et al.,
591 2021)²⁴). LandScan data may be underestimated in urban-rural transition zones and
592 overestimated in sparsely populated areas (Beata et al., 2019). Nevertheless, OSM road
593 data remain the only globally available open data source that includes road surface type
594 labels; GHSL and LandScan data are also globally ~~covered~~comprehensive, freely
595 accessible geospatial data products with long time series, which is why this study
596 selected these data for experimental analysis. However, in the future, other data sources
597 (e.g., CORINE Land Cover (Pontius Jr et al., 2017), World Settlement Footprint
598 (Marconcini et al., 2020), and Global Human Settlement Population Grid (Yin et al.,
599 2021)) could be considered, and their impact on the quality of road surface type dataset
600 could be analyzed.

601

602 5.2 Implications and Significance

603 Compared to traditional statistical data such as those from IRF, the first-ever road
604 surface type dataset for 50 African countries and regions developed in this study not
605 only ~~allows for~~enables the calculation of statistical indicators such as paved road length
606 and road paved rate for each country and region but also ~~enables~~facilitates detailed
607 ~~analysis~~analyses of which roads are paved or unpaved, ~~providing~~This provides
608 ~~valuable~~decision-making support for improving local transportation infrastructure (e.g.,
609 ~~upgrading unpaved roads to paved~~roads~~ones~~). Additionally, road surface types ~~are~~serve
610 ~~as~~an important data source for assessing SDG 9.1. Therefore, this dataset can also be

设置了格式: 突出显示
带格式的: 缩进: 首行缩进: 0 厘米

设置了格式: 突出显示

设置了格式: 突出显示

设置了格式: 突出显示

设置了格式: 突出显示

设置了格式: 突出显示

设置了格式: 突出显示

611 combined with population and urban built-up area data to analyze the proportion of
612 rural populations within 2 km of paved or unpaved roads in various African countries
613 (Wanjing et al., 2021), to provide data support for evaluating Africa's sustainable
614 development goals. Last but not least, this dataset can be combined with location data
615 of traffic accidents to analyze the relationship between road surface types and traffic
616 accidents (Patrick et al., 2022); with traffic carbon emission data to analyze the
617 relationship between road surface types and environmental impacts (Ling et al., 2024);
618 or with national income data to analyze the relationship between road surface types and
619 socioeconomic development (Anyanwu et al., 2009).

620 Moreover, this study utilized multisource geospatial big data and deep learning
621 models to develop the African road surface type dataset. The primary advantage of this
622 method is that its source data (including OSM, LandScan, GDP, GHSL-BUILT, and
623 ESRI Land Cover) are not only openly accessible but also globally covered. Therefore,
624 this method ~~could also can~~ be applied to identify road surface types in other countries
625 and regions worldwide, providing methodological support for ~~developing the~~
626 development of a global road surface type dataset.

627 5.3 Limitations and future work

628 (1) This study adopted the method proposed by Zhou et al. (2025b) to develop the
629 African road surface type dataset. This method designs 16 proxy indicators across three
630 dimensions (Road network, Socioeconomic, and Geographical Environment) from five
631 types of open geospatial data to infer road surface types. In the future, other additional
632 data sources such as terrain data could be introduced, and incorporated, as unpaved

带格式的: 缩进: 首行缩进: 0 厘米

设置了格式: 突出显示

设置了格式: 突出显示

设置了格式: 突出显示

设置了格式: 突出显示

633 roads are likely common in mountainous areas due to high construction costs. Thus,
634 additional proxy indicators such as (e.g. elevation and slope, aspect, and surface
635 roughness could) may be designed/considered to investigate/determine whether these
636 indicators they can improve/enhance the classification accuracy of the data product.

设置了格式: 突出显示
设置了格式: 突出显示

637 (2) Road surface types are not limited to just paved and unpaved roads; they can
638 also be further subdivided into categories such as asphalt, concrete, and dirt roads.
639 However, we found that most paved roads in Africa are asphalt roads, and most unpaved
640 roads are dirt roads; thus; therefore, this study only considered "the "paved"" and
641 "unpaved"" categories. Nevertheless, in the future, by supplementing field-measured
642 data, it could/may be explored/possible to explore whether this method can be used to
643 develop dataset that include more detailed road surface type classifications.

644 (3) The African road surface type dataset developed in this study is limited to a
645 single year, approximately 2020. This is because the source data used were all obtained
646 from 2020 or nearby years to ensure temporal consistency across (i.e., 2018 or 2019).
647 Although existing studies have reported that GDP and building height data change little
648 within a period of 1-2 years (African Development Bank Group, 2020; Ali et al., 2025),
649 inconsistencies in the years may still affect the quality of our dataset for different
650 African countries. Therefore, it is worthwhile to investigate whether the quality of the
651 road surface type dataset could be improved by using source data obtained from the
652 same year.

设置了格式: 字体: +西文正文 (等线), 五号
设置了格式: 突出显示
设置了格式: 突出显示

653 (4) Although most open geospatial big data (such as OSM, GDP, and population
654 data) include data/information from different years, which could potentially be used to

设置了格式: 突出显示

655 develop road surface type dataset for multiple years, validation data are difficult to
656 obtain. Specifically, it is challenging to interpret roads and their surface types using
657 open-source medium- to low-resolution satellite imagery (e.g., Landsat or Sentinel-2).
658 Although Google satellite imagery has offers higher resolution, the update years of
659 Google imagery for different areas within a country may not be consistent, making it
660 difficult to analyze changes in road surface types. Nonetheless, in the future, this
661 method could be attempted to develop road surface type dataset for different years, and
662 accuracy could be validated using long-time-series high-resolution remote sensing
663 imagery; further, spatiotemporal changes in road surface types at a large scale could be
664 analyzed.

665

666 **6. Data availability**

667 — The First Road Surface Dataset for 50 African countries and reigns is distributed
668 under the CC BY 4.0 License. The data can be downloaded from the data repository
669 Figshare at <https://doi.org/10.6084/m9.figshare.29424107> (Liu et al., 2025).

670

671 **7. Conclusion**

672 This study developed the first dataset containing road surface types for every road in
673 50 African countries and regions, based on multi-source geospatial data and deep
674 learning model. The accuracy of this dataset was evaluated through visual interpretation
675 using high-resolution Google satellite imagery and Google street view, while its
676 effectiveness was indirectly analyzed by comparing it with IRF statistical data and

677 socio-economic indicators such as HDI and GNI per capita. Finally, the spatial
678 distribution patterns of road surface types across these 50 African countries and regions
679 were analyzed using the developed dataset. The main findings are as follows:

680 (1) The accuracy of the road surface type dataset for ~~the~~ 50 African countries and
681 regions ranges from 77% to 96%, with F1 scores between 0.76 and 0.96, validating the
682 effectiveness of the developed dataset.

683 (2) In terms of total road length, paved road length, and road paved rate, the
684 correlation coefficients between ~~the~~-calculations based on our dataset and the IRF
685 statistical data ~~show high demonstrate a strong~~ correlation, ranging from 0.69 to 0.94.

686 Regarding socio-economic indicators (GNI per capita and HDI), the calculations based
687 on our dataset also exhibit high correlation with the relevant statistical data, ranging
688 from 0.80 to 0.83, indirectly verifying the effectiveness of our dataset.

689 (3) From a spatial perspective, the road paved rate in Africa is generally low. The
690 average road paved rate across the 50 African countries and regions is only 17.4%,
691 ~~displaying exhibiting~~ a spatial pattern of ~~"~~higher in the north and south, lower in the
692 central region~~"~~. Specifically, the average road paved rate in ~~the north of Saharan North~~
693 Africa is approximately ~~3~~three times that of Sub-Saharan Africa (excluding South
694 Africa).

695 The dataset developed in this study includes the surface type of every road in Africa,
696 ~~offering providing valuable support for~~ decision-making ~~support for aimed at~~ improving
697 the region's road infrastructure. Additionally, this dataset can be combined with data on
698 population and urban built-up areas to assess Africa's Sustainable Development Goals

699 (e.g., SDG 9.1). Furthermore, it can be integrated with other datasets—such as [those on](#)
700 traffic accidents, carbon emissions, and national income—to analyze the impact of road
701 surface types on road safety, energy consumption, ecological environment, and socio-
702 economic development.

703

704 **Author contributions** ZL developed the data and wrote the original manuscript. QZ
705 proposed methods and designed experiments. FZ reviewed and improved the
706 manuscript. LP checked and validated data quality. All authors discussed and improved
707 the manuscript.

708

709 **Competing interests** The contact author has declared that none of the authors has
710 any competing interests.

711

712 **Acknowledgements** The project was supported by National Natural Science
713 Foundation of China (Grant No. 42471492).

714

715 **References**

716 [Abdulkadr, A.A., Juma, L.O., Gogo, A.F., Neszmélyi, G.I. East African Transport](#) 带格式的: 缩进: 首行缩进: 2 字符

717 [Infrastructure: The Cases of Ethiopia, Kenya and Tanzania. Reg. Econ. South Russ.,](#)

718 [10\(4\): 89–102, 2022.](#)

719 [African Union Commission Agenda 2063. African Union Policy Doc., 2015.](#) 带格式的: 缩进: 首行缩进: 0.74 厘米

720 [African Development Bank Group. African Economic Outlook 2020: Developing](#)

721 [Africa's Workforce for the Future. African Development Bank, 2020.](#)

722 [Ali, S., Alireza, D., Parviz, A. Volumetric insights into urban growth analysis: Investigating vertical and horizontal patterns. Sustainable Cities and Society. Volume 130, 106589, ISSN 2210-6707, 2025.](#)

725 Anyanwu, J.C., Erhijakpor, A.E.O. The Impact of Road Infrastructure on Poverty Reduction in Africa. In: Poverty in Africa (Ed. T.W. Beasley), 1–40, 2009.

727 [Arik, S.Ö., Pfister, T. Tabnet: Attentive Interpretable Tabular Learning. Proc. AAAI Conf. Artif. Intell., 35\(8\): 6679 – 6687, <https://doi.org/10.48550/arXiv.1908.07442>, 2021.](#)

730 [Baak, M., Koopman, R., Snoek, H., Klous, S. A new correlation coefficient between categorical, ordinal and interval variables with Pearson characteristics. Comput. Stat. Data Anal., 152: 107043, <https://doi.org/10.1016/j.csda.2020.107043>, 2020.](#)

734 [Barrington-Leigh, C., Millard-Ball, A. The World's User-Generated Road Map Is More Than 80% Complete. PLoS ONE. 12\(8\): e0180698, <https://doi.org/10.1371/journal.pone.0180698>, 2017.](#)

737 [Biber-Freudenberger, L., Christina, B., Georg, B., et al. Impacts of road development in sub-Saharan Africa: A call for holistic perspectives in research and policy. iScience, 28\(2\): 111913, <https://doi.org/10.1016/j.isci.2025.111913>, 2025.](#)

740 [Calka, B., Bielecka, E. Reliability Analysis of LandScan Gridded Population Data. The Case Study of Poland. ISPRS Int. J. Geo-Inf., 8\(5\): 222, <https://doi.org/10.3390/ijgi8050222>, 2019.](#)

带格式的: 缩进: 首行缩进: 0.74 厘米

743 [Central Intelligence Agency \(CIA\) The World Factbook. CIA Publ., 2023.](#)
744 [Chen, J., Gao, M., Cheng, S., Hou, W., Song, M., Liu, X., Liu, Y. Global 1 Km × 1](#)
745 [Km Gridded Revised Real Gross Domestic Product and Electricity Consumption](#)
746 [During 1992–2019 Based on Calibrated Nighttime Light Data. Sci. Data, 9\(1\): 202,](#)
747 [<https://doi.org/10.1038/s41597-022-01322-5>, 2022.](#)
748 [Chen, K., Tan, G., Lu, M., Wu, J. CRSM: A Practical Crowdsourcing-Based Road](#)
749 [Surface Monitoring System. Wirel. Netw., 22: 765 – 779,](#)
750 [<https://doi.org/10.1007/s11276-015-0996-y>, 2016.](#)
751 [Chen, Y., Li, C., Wang, W., et al. The Landscape, Trends, Challenges, and](#)
752 [Opportunities of Sustainable Mobility and Transport. npj Sustain. Mobil. Transp., 2: 8,](#)
753 [<https://doi.org/10.1038/s44333-025-00026-8>, 2025.](#)
754 [Dobson, J.E., Bright, E.A., Coleman, P.R., Durfee, R.C., Worley, B.A. Landscan:](#)
755 [A Global Population Database for Estimating Populations at Risk. Photogramm. Eng.](#)
756 [Remote Sens., 66\(7\): 849–857, 2000.](#)
757 [Greening, T., O'Neill, P. Traffic Generated Dust from Unpaved Roads: An](#)
758 [Overview of Impacts and Options for Control. Proc. 1st AFCAP Pract. Conf., 23–25](#)
759 [Nov 2010, 2010.](#)
760 [Gwilliam, K., Foster, V., Archondo-Callao, R., Briceño-Garmendia, C., Nogales,](#)
761 [A., Sethi, K. The Burden of Maintenance: Roads in Sub-Saharan Africa. Africa](#)
762 [Infrastruct. Ctry. Diagn., 14\(1\), 2008.](#)
763 [Harikrishnan, P.M., Gopi, V.P. Vehicle Vibration Signal Processing for Road](#)
764 [Surface Monitoring. IEEE Sens. J., 17\(16\): 5192 – 5197.](#)

765 [https://doi.org/10.1109/JSEN.2017.2719865, 2017.](https://doi.org/10.1109/JSEN.2017.2719865)

766 Jiang, S., Zhang, Z., Ren, H., Wei, G., Xu, M., Liu, B. Spatiotemporal

767 Characteristics of Urban Land Expansion and Population Growth in Africa from 2001

768 to 2019: Evidence from Population Density Data. ISPRS Int. J. Geo-Inf., 10(9): 584,

769 [https://doi.org/10.3390/ijgi10090584, 2021.](https://doi.org/10.3390/ijgi10090584)

770 Karra, K., Kontgis, C., Statman-Weil, Z., Mazzariello, J., Mathis, M., Brumby, S.

771 Global Land Use/Land Cover with Sentinel-2 and Deep Learning. Proc. IEEE IGARSS,

772 4704–4707, [https://doi.org/10.1109/IGARSS47720.2021.9553499, 2021.](https://doi.org/10.1109/IGARSS47720.2021.9553499)

773 Kresnanto, N.C. Model of Relationship Between Car Ownership Growth and

774 Economic Growth in Java. IOP Conf. Ser. Mater. Sci. Eng., 650: 012047,

775 [https://doi.org/10.1088/1757-899X/650/1/012047, 2019.](https://doi.org/10.1088/1757-899X/650/1/012047)

776 Li, W., Zhou, Q., Zhang, Y., Chen, Y. Visualising Rural Access Index and Not

777 Served Rural Population in Africa. Environ. Plan. A Econ. Space, 54(2): 215–218,

778 [http://doi.org/10.1177/0308518X211035786, 2022.](http://doi.org/10.1177/0308518X211035786)

779 Li, W., Zhou, Q., Zhang, Y., Chen, Y. Visualizing Rural Access Index and Not

780 Served Rural Population in Africa. Environ. Plan. A Econ. Space, 54(2): 215–218,

781 [https://doi.org/10.1177/0308518X211035786, 2022.](https://doi.org/10.1177/0308518X211035786)

782 Li, X., Goldberg, D.W. Toward a Mobile Crowdsensing System for Road Surface

783 Assessment. Comput. Environ. Urban Syst., 69: 51 – 62,

784 [https://doi.org/10.1016/j.compenvurbsys.2017.12.005, 2018.](https://doi.org/10.1016/j.compenvurbsys.2017.12.005)

785 Ling, C., Tang, J., Zhao, P., Xu, L., Lu, Q., Yang, L., Huang, F., Lyu, W., Yang, J.

786 Unraveling the Relation Between Carbon Emission and Carbon Footprint: A Literature

787 [Review and Framework for Sustainable Transportation. *npj Sustain. Mobil. Transp.*, 1: 13, https://doi.org/10.1038/s44333-024-00013-5, 2024.](https://doi.org/10.1038/s44333-024-00013-5)

788 [Liu, Z., Qi, Z.: The First Road Surface Type Dataset for 50 African Countries and Regions, Figshare \[data set\], https://doi.org/10.6084/m9.figshare.29424107, 2025.](https://doi.org/10.6084/m9.figshare.29424107)

789 [Louhghalam, A., Akbarian, M., Ulm, F.J. Roughness-Induced Pavement–Vehicle Interactions: Key Parameters and Impact on Vehicle Fuel Consumption. *Transp. Res. Rec.*, 2525\(1\): 62–70, 2015.](https://doi.org/10.1007/s11341-015-0925-2)

790 [Marconcini, M., Metz-Marconcini, A., Üreyen, S., et al. Outlining where humans live, the World Settlement Footprint 2015. *Sci. Data*, 7: 242, https://doi.org/10.1038/s41597-020-00580-5, 2020.](https://doi.org/10.1038/s41597-020-00580-5)

791 [Menegazzo, J., von Wangenheim, A. Multi-Contextual and Multi-Aspect Analysis for Road Surface Type Classification Through Inertial Sensors and Deep Learning. *Proc. IEEE SBESC*, 1–8, https://doi.org/10.1109/SBESC51047.2020.9277846, 2020.](https://doi.org/10.1109/SBESC51047.2020.9277846)

792 [Mohit, P.M., Slobodan, P.S. Understanding dynamics of population flood exposure in Canada with multiple high-resolution population datasets. *Sci. Total Environ.*, 759: 143559, https://doi.org/10.1016/j.scitotenv.2020.143559, 2021.](https://doi.org/10.1016/j.scitotenv.2020.143559)

793 [Patrick, M., Yves, A. Access to Paved Roads, Gender, and Youth Unemployment in Rural Areas: Evidence from Sub-Saharan Africa. *Afr. Dev. Rev.*, 35\(2\): 165–180, https://doi.org/10.1111/1467-8268.12701, 2022.](https://doi.org/10.1111/1467-8268.12701)

794 [Pérez-Fortes, A.P., Giudici, H. A Recent Overview of the Effect of Road Surface Properties on Road Safety, Environment, and How to Monitor Them. *Environ. Sci. Pollut. Res.*, 29\(44\): 65993–66009, https://doi.org/10.1007/s11356-022-21847-x, 2022.](https://doi.org/10.1007/s11356-022-21847-x)

带格式的: 缩进: 首行缩进: 0.74 厘米

809 Pesaresi, M., Corbane, C., Ren, C., Edward, N. Generalized Vertical Components
810 of Built-Up Areas from Global Digital Elevation Models by Multi-Scale Linear
811 Regression Modelling. PLoS ONE, 16(2): e0244478,
812 <https://doi.org/10.1371/journal.pone.0244478>, 2021.
813 Pontius Jr, R.G. European Landscape Dynamics: Corine Land Cover Data.
814 Photogramm. Eng. Remote Sens., 83(2): 79, <https://doi.org/10.1201/9781315372860>,
815 2017.
816 Randhawa, S., Eren, A., Guntaj, R., Herfort, B., Lautenbach, Sven., Zipf, A. Paved or
817 unpaved? A deep learning derived road surface global dataset from Mapillary Street-
818 View Imagery. ISPRS J. Photogramm. Remote Sens., 223: 1 – 14,
819 <https://doi.org/10.1016/j.isprsjprs.2025.02.020>, 2025.
820 Sattar, S., Li, S., Chapman, M. Road Surface Monitoring Using Smartphone → 带格式的: 缩进: 首行缩进: 0.74 厘米
821 Sensors: A Review. Sensors, 18(11): 3845, <https://doi.org/10.3390/s18113845>, 2018.
822 Sha, A. Advances and Development Trends in Eco-friendly Pavements. J. Road Eng.,
823 1: 1–42, <https://doi.org/10.1016/j.jreng.2021.12.002>, 2021.
824 Shtayat, A., Moridpour, S., Best, B. A Review of Monitoring Systems of Pavement → 带格式的: 缩进: 首行缩进: 0.74 厘米
825 Condition in Paved and Unpaved Roads. J. Traffic Transp. Eng., 7(5): 629–638,
826 <https://doi.org/10.1016/j.jtte.2020.03.004>, 2020.
827 Sha, A. Advances and Development Trends in Eco-friendly Pavements. J. Road Eng.,
828 1: 1–42, <https://doi.org/10.1016/j.jreng.2021.12.002>, 2021.
829 Styer, J., Tunstall, L., Landis, A.E., Grenfell, J. Innovations in Pavement Design → 带格式的: 缩进: 首行缩进: 0.74 厘米
830 and Engineering: A 2023 Sustainability Review. Heliyon, 10(13): e33481,

831 <https://doi.org/10.1016/j.heliyon.2024.e33602>; <https://doi.org/10.1016/j.heliyon.2024.e33602>, 2024.

832 <https://doi.org/10.1038/s44333-025-00026-8>, 2025.

833 <https://doi.org/10.1038/s44333-025-00026-8>, 2025.

834 <https://doi.org/10.1038/s44333-025-00026-8>, 2025.

835 <https://doi.org/10.1038/s44333-025-00026-8>, 2025.

836 <https://doi.org/10.1038/s44333-025-00026-8>, 2025.

837 <https://doi.org/10.1038/s44333-025-00026-8>, 2025.

838 <https://doi.org/10.1038/s44333-025-00026-8>, 2025.

839 <https://doi.org/10.1038/s44333-025-00026-8>, 2025.

840 <https://doi.org/10.1038/s44333-025-00026-8>, 2025.

841 <https://doi.org/10.1038/s44333-025-00026-8>, 2025.

842 <https://doi.org/10.1038/s44333-025-00026-8>, 2025.

843 <https://doi.org/10.1038/s44333-025-00026-8>, 2025.

844 <https://doi.org/10.1038/s44333-025-00026-8>, 2025.

845 <https://doi.org/10.1038/s44333-025-00026-8>, 2025.

846 <https://doi.org/10.1038/s44333-025-00026-8>, 2025.

847 <https://doi.org/10.1038/s44333-025-00026-8>, 2025.

848 <https://doi.org/10.1038/s44333-025-00026-8>, 2025.

849 <https://doi.org/10.1038/s44333-025-00026-8>, 2025.

850 <https://doi.org/10.1038/s44333-025-00026-8>, 2025.

851 <https://doi.org/10.1038/s44333-025-00026-8>, 2025.

852 <https://doi.org/10.1038/s44333-025-00026-8>, 2025.

带格式的: 缩进: 首行缩进: 2 字符

带格式的: 缩进: 首行缩进: 0.74 厘米

853 <https://doi.org/10.1111/1467-8268.12701>, 2022.

854 Barrington-Leigh, C., Millard-Ball, A. The World's User Generated Road Map Is

855 More Than 80% Complete. *PLoS ONE*, 12(8): e0180698,

856 <https://doi.org/10.1371/journal.pone.0180698>, 2017.

857 Central Intelligence Agency (CIA) *The World Factbook*. CIA Publ., 2023.

858 Turner, B. International Road Federation (IRF). *Statesman's Yearb.*, 2015: 49–50,

859 2014.

860 Louighalam, A., Akbarian, M., Ulm, F.J. *Roughness Induced Pavement-Vehicle*

861 *Interactions: Key Parameters and Impact on Vehicle Fuel Consumption*. *Transp. Res. Res.*, 2525(1): 62–70, 2015.

863 Sattar, S., Li, S., Chapman, M. *Road Surface Monitoring Using Smartphone*

864 *Sensors: A Review*. *Sensors*, 18(11): 3845, <https://doi.org/10.3390/s18113845>, 2018.

865 Pérez Fortes, A.P., Giudicei, H. *A Recent Overview of the Effect of Road Surface*

866 *Properties on Road Safety, Environment, and How to Monitor Them*. *Environ. Sci. Pollut. Res.*, 29(44): 65993–66009, <https://doi.org/10.1007/s11356-022-21847-x>, 2022.

868 Chen, K., Tan, G., Lu, M., Wu, J. *CRSM: A Practical Crowdsourcing-Based Road*

869 *Surface Monitoring System*. *Wirel. Netw.*, 22: 765–779,

870 <https://doi.org/10.1007/s11276-015-0996-y>, 2016.

871 Harikrishnan, P.M., Gopi, V.P. *Vehicle Vibration Signal Processing for Road*

872 *Surface Monitoring*. *IEEE Sens. J.*, 17(16): 5192–5197,

873 <https://doi.org/10.1109/JSEN.2017.2719865>, 2017.

874 Li, X., Goldberg, D.W. *Toward a Mobile Crowdsensing System for Road Surface*

875 Assessment. Comput. Environ. Urban Syst., 69: 51–62,
876 <https://doi.org/10.1016/j.compenvurbys.2017.12.005>, 2018.

877 Randhawa, S., Eren, A., Guntur, R., Herfort, B., Lautenbacher, Sven., Zipf, A. Paved or
878 unpaved? A deep learning derived road surface global dataset from Mapillary Street
879 View Imagery. ISPRS J. Photogramm. Remote Sens., 223: 1–14,
880 <https://doi.org/10.1016/j.isprsjprs.2025.02.020>, 2025.

881 Menegazzo, J., von Wangenheim, A. Multi-Contextual and Multi-Aspect Analysis → 带格式的: 缩进: 首行缩进: 0.74 厘米
882 for Road Surface Type Classification Through Inertial Sensors and Deep Learning. Proc.
883 IEEE SBESC, 1–8, <https://doi.org/10.1109/SBESC51047.2020.9277846>, 2020.

884 Zhou, Q., Duan, J., Qiao, J., Liu, Z., Yang, H. A Large Crowdsourced Street View
885 Dataset for Mapping Road Surface Types in Africa. Sci. Data, 12: 1003,
886 <https://doi.org/10.1038/s41597-025-05153-y>, 2025a.

887 Workman, R., Wong, P., Wright, A., Wang, Z. Prediction of Unpaved Road
888 Conditions Using High-Resolution Optical Satellite Imagery and Machine Learning.
889 Remote Sens., 15(16): 3985, <https://doi.org/10.3390/rs15163985>, 2023.

890 World Bank First African Observatory to Tackle the Continent's Road Safety Crisis.
891 World Bank Press Release, 23 May 2018, 2018a.

892 Yan, M., Pang, Y., He, Y., Meng, S. Consistency Analysis and Accuracy Evaluation
893 of Multi-Source Land Cover Products in Pu'er. For. Resour. Manag., (1): 173–182,
894 <https://doi.org/10.13466/j.cnki.lyzygl.2023.01.020>, 2023.

895 Yeh, C., Perez, A., Driscoll, A., Jepson, G., Cotton, A., Wang, Z., Ermon, S., Burke,
896 M., Lobell, D. Using publicly available satellite imagery and deep learning to

897 [understand economic well-being in Africa. Nature Communications, 11\(1\): 2583, 2020.](#)

898 [Zhou, Q., Liu, Z., Huang, Z. Mapping Road Surface Type of Kenya Using](#)

带格式的: 缩进: 首行缩进: 0.74 厘米

899 [OpenStreetMap and High-resolution Google Satellite Imagery. Sci. Data, 11: 331,](#)

900 [<https://doi.org/10.1038/s41597-024-03158-7>, 2024.](#)

901 [Zhou, Q., Liu, Y., Liu, Z. Mapping National-Scale Road Surface Types Using](#)

902 [Multisource Open Data and Deep Learning Model. Trans. GIS, 29\(1\): 123–141,](#)

903 [<https://doi.org/10.1111/tgis.13305>, 2025.](#)

904 [Biber-Freudenberger, L., Christina, B., Georg, B., et al. Impacts of road](#)

905 [development in sub-Saharan Africa: A call for holistic perspectives in research and](#)

906 [policy. iScience, 28\(2\): 111913, <https://doi.org/10.1016/j.isci.2025.111913>, 2025.](#)

907 [Chen, J., Gao, M., Cheng, S., Hou, W., Song, M., Liu, X., Liu, Y. Global 1 Km × 1](#)

908 [Km Gridded Revised Real Gross Domestic Product and Electricity Consumption](#)

909 [During 1992–2019 Based on Calibrated Nighttime Light Data. Sci. Data, 9\(1\): 202,](#)

910 [<https://doi.org/10.1038/s41597-022-01322-5>, 2022.](#)

911 [Dobson, J.E., Bright, E.A., Coleman, P.R., Durfee, R.C., Worley, B.A. LandScan:](#)

912 [A Global Population Database for Estimating Populations at Risk. Photogramm. Eng.](#)

913 [Remote Sens., 66\(7\): 849–857, 2000.](#)

914 [Yin, X., Li, P., Feng, Z., Yang, Y., You, Z., Xiao, C. Which Gridded Population](#)

915 [Data Product Is Better? Evidences from Mainland Southeast Asia \(MSEA\). ISPRS Int.](#)

916 [J. Geo-Inf., 10\(10\): 681, <https://doi.org/10.3390/ijgi10100681>, 2021.](#)

917 [Zhou, Q., Duan, J., Qiao, J., Liu, Z., Yang, H. A Large Crowdsourced Street View](#)

918 [Dataset for Mapping Road Surface Types in Africa. Sci. Data, 12: 1003,](#)

919 <https://doi.org/10.1038/s41597-025-05153-y>, 2025a.

920 Mohit, P.M., Slobodan, P.S. Understanding dynamics of population flood exposure
921 in Canada with multiple high resolution population datasets. *Sci. Total Environ.*, 759,
922 143559, <https://doi.org/10.1016/j.scitotenv.2020.143559>, 2021.

923 Jiang, S., Zhang, Z., Ren, H., Wei, G., Xu, M., Liu, B. Spatiotemporal
924 Characteristics of Urban Land Expansion and Population Growth in Africa from 2001
925 to 2019: Evidence from Population Density Data. *ISPRS Int. J. Geo-Inf.*, 10(9): 584,
926 <https://doi.org/10.3390/ijgi10090584>, 2021.

927 Pesaresi, M., Corbane, C., Ren, C., Edward, N. Generalized Vertical Components
928 of Built Up Areas from Global Digital Elevation Models by Multi-Scale Linear
929 Regression Modelling. *PLoS ONE*, 16(2): e0244478,
930 <https://doi.org/10.1371/journal.pone.0244478>, 2021.

931 Karras, K., Kontgis, C., Statman-Weil, Z., Mazzariello, J., Mathis, M., Brumby, S.
932 Global Land Use/Land Cover with Sentinel-2 and Deep Learning. *Proc. IEEE IGARSS*,
933 4704–4707, <https://doi.org/10.1109/IGARSS47720.2021.9553499>, 2021.

934 Van, M., Pang, Y., He, Y., Meng, S. Consistency Analysis and Accuracy Evaluation of
935 Multi-Source Land Cover Products in Pu'er. *For. Resour. Manag.*, (1): 173–182,
936 <https://doi.org/10.13466/j.enki.lyzygl.2023.01.020>, 2023.

937 Zhou, Q., Li, Z. A comparative study of various strategies to concatenate road
938 segments into strokes for map generalization. *Int. J. Geogr. Inf. Sci.*, 26(4): 691–715,
939 <https://doi.org/10.1080/13658816.2011.609990>, 2012.

940 Zhou, Q., Li, Z. How many samples are needed? An investigation of binary logistic

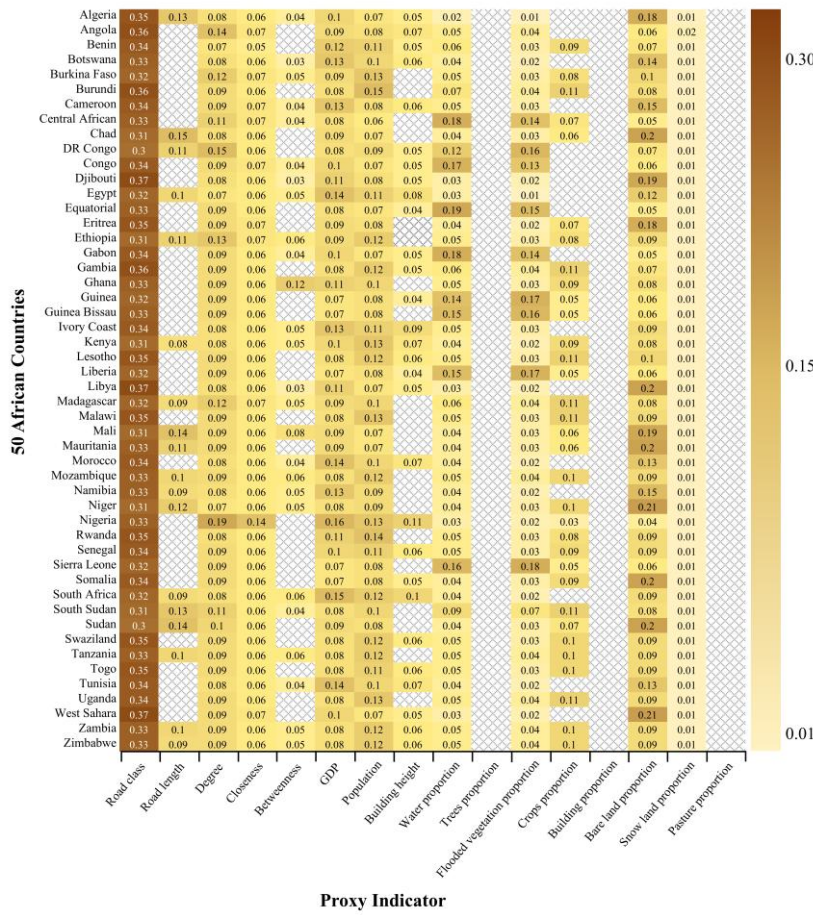
带格式的: 缩进: 首行缩进: 0.74 厘米

941 [regression for selective omission in a road network, Cartography and Geographic](#)
942 [Information Science. 1545-0465, 20 Nov, 2015](#)
943 [Zhou, Q., Liu, Y., Liu, Z. Mapping National-Scale Road Surface Types Using](#) 带格式的: 缩进: 首行缩进: 0.74 厘米
944 [Multisource Open Data and Deep Learning Model. Trans. GIS, 29\(1\): 123–141,](#)
945 [https://doi.org/10.1111/tgis.13305, 2025b.](#)
946 [Zhou, Q., Liu, Z., Huang, Z. Mapping Road Surface Type of Kenya Using](#)
947 [OpenStreetMap and High-resolution Google Satellite Imagery. Sci. Data, 11: 331,](#)
948 [https://doi.org/10.1038/s41597-024-03158-7, 2024.](#)
949 [Zhou, Q., Baak, M., Koopman, R., Snoek, H., Klous, S. A new correlation](#)
950 [coefficient between categorical, ordinal and interval variables with Pearson](#)
951 [characteristics. Comput. Stat. Data Anal., 152: 107043,](#)
952 [https://doi.org/10.1016/j.csda.2020.107043, 2020.](#)
953 [Arik, S.Ö., Pfister, T. Tabnet: Attentive Interpretable Tabular Learning. Proc. AAAI](#)
954 [Conf. Artif. Intell., 35\(8\): 6679–6687, https://doi.org/10.48550/arXiv.1908.07442,](#)
955 [2021.](#)
956 [Gwilliam, K., Foster, V., Archondo Callao, R., Briceño Carmendia, C., Nogales,](#)
957 [A., Sethi, K. The Burden of Maintenance: Roads in Sub-Saharan Africa. Africa](#)
958 [Instruct. Ctry. Diagn., 14\(1\), 2008.](#)
959 [Zhou, Q., Wang, S., Liu, Y. Exploring the accuracy and completeness patterns of](#)
960 [global land-cover/land-use data in OpenStreetMap. Appl. Geogr., 145: 102742,](#)
961 [https://doi.org/10.1016/j.apgeog.2022.102742, 2022.](#)

962

Appendix A

963 This figure shows the selected proxy indicators for 50 African countries. For each
 964 country, each value in the grid represents the mean SHAP of the corresponding proxy
 965 indicator (e.g., road class). Darker colors indicate higher contributions to the
 966 classification results. Empty values mean that the corresponding proxy indicator was
 967 not used for model training, because it has a high correlation (> 0.7) with at least one
 968 other proxy indicator but its mean SHAP is lower.



969

970 [Figure A1. The Selected Proxy Indicators For 50 African Countries](#) Calka, B.,

带格式的: 缩进: 首行缩进: 0.74 厘米

971 Bielecka, E. Reliability Analysis of LandScan Gridded Population Data. The Case

972 Study of Poland. *ISPRS Int. J. Geo Inf.*, 8(5): 222, <https://doi.org/10.3390/ijgi8050222>,

973 2019.

974 Pontius Jr., R.G. European Landscape Dynamics: Corine Land Cover Data.

975 *Photogramm. Eng. Remote Sens.*, 83(2): 79, <https://doi.org/10.1201/9781315372860>,

976 2017.

977 Marconeini, M., Metz Marconeini, A., Üreyen, S., et al. Outlining where humans

978 live, the World Settlement Footprint 2015. *Sci. Data.*, 7: 242,

979 <https://doi.org/10.1038/s41597-020-00580-5>, 2020.

980 Li, W., Zhou, Q., Zhang, Y., Chen, Y. Visualizing Rural Access Index and Not

981 Served Rural Population in Africa. *Environ. Plan. A Econ. Space*, 54(2): 215–218,

982 <https://doi.org/10.1177/0308518X211035786>, 2022.

983 Ling, C., Tang, J., Zhao, P., Xu, L., Lu, Q., Yang, L., Huang, F., Lyu, W., Yang, J.

984 Unraveling the Relation Between Carbon Emission and Carbon Footprint: A Literature

985 Review and Framework for Sustainable Transportation. *npj Sustain. Mobil. Transp.*, 1:

986 13, <https://doi.org/10.1038/s44333-024-00013-5>, 2024.

987 Liu, Z., Qi, Z.: The First Road Surface Type Dataset for 50 African Countries and

带格式的: 居中

988 Regions, Figshare [data set], <https://doi.org/10.6084/m9.figshare.29424107>, 2025.